GRAPHICAL MODELS AND IMAGE PROCESSING
Vol. 59, No. 5, September, pp. 310–320, 1997
ARTICLE NO. IP970435

Identification of Blur Parameters from Motion Blurred Images

Y. Yitzhaky[1] and N. S. Kopeika[2]

Department of Electrical and Computer Engineering, Ben-Gurion University of the Negev, P.O. Box 653, Beer Sheva, 84105 Israel

Received April 10, 1996; revised April 30, 1997; accepted May 8, 1997

The problem of restoration of images blurred by relative motion between the camera and the object scene is important in a large number of applications. The solution proposed here identifies important parameters with which to characterize the point spread function (PSF) of the blur, given only the blurred image itself. This identification method is based on the concept that image characteristics along the direction of motion are different from the characteristics in other directions. Depending on the PSF shape, the homogeneity and the smoothness of the blurred image in the motion direction are greater than in other directions. Furthermore, in this direction correlation exists between the pixels forming the blur of the original unblurred objects. By filtering the blurred image we emphasize the PSF characteristics at the expense of the image characteristics. The method proposed here identifies the direction and the extent of the PSF of the blur and evaluates its shape which depends on the type of motion during the exposure. Correct identification of the PSF parameters permits fast high resolution restoration of the blurred image. © 1997 Academic Press

1. INTRODUCTION

A difficult problem for imaging systems is degradation of images caused by motion. This problem is common when the imaging system is in moving vehicles such as tanks or planes and even when the camera is held by human hands. The quality and reliability of the image restoration process is usually based on the accuracy of information concerning the degradation process.

For a given ideal picture $f(x, y)$, the corresponding degraded picture $g(x, y)$ is often modeled as

$$g(x, y) = \int\int h(x - x', y - y') f(x', y')\, dx'\, dy' + n(x, y) \tag{1}$$

where $h(x, y)$ is a linear shift-invariant PSF (point spread function) and $n(x, y)$ is random noise.

In motion-blurred images, the blur extent parameter is the smear extent of the blurred image of a point object in the original image. Extraction of the blur extent has significant meaning in identification of the motion-blur PSF. Cannon [1] dealt with the case of uniform linear motion blur that is described by a square pulse PSF and used its property of periodic zeros in the spectral domain of the blurred image. These zeros were emphasized in the *cepstral* domain and the blur extent was estimated by measuring the separations between the zeros. The assumption of zeros in the spectral domain is not satisfied in various cases of motion degradation such as accelerated motion [2, 3] and low frequency vibrations [4].

Recent important developments in image restoration are the maximum likelihood image and blur identification methods [5–7]. These methods model the original image, the blur, and the noise process. The original image is modeled as a two-dimensional autoregressive (AR) process, and the blur is modeled by a two-dimensional linear system with finite impulse response. A maximum likelihood estimation is used for identification of the image and blur parameters. The identification of the blur model parameters is incorporated into the restoration algorithm and require many computations.

Savakis and Trussell [8] suggested another blur identification method. Using an estimation of the original image power spectrum (an expected value), the PSF estimate is chosen from a collection of candidate PSFs to provide the best match between the restoration residual power spectrum and the expected residual spectrum given that the candidate PSF is similar to the true PSF.

In this paper we develop a new method for identifying blur parameters from the motion blurred image itself. Based on investigation of the motion blurring effects on the image, blur characteristics such as direction, extent, and shape estimation are extracted from the blurred image. Although the motivation for blur identification is usually image restoration, the method proposed here does not relate the identification process to the restoration process. The method addresses one-dimensional blur types, which are common in the case of motion degradation. The blur effect is assumed to be linear and space invariant and

[1] E-mail: itzik@newton.bgu.ac.il.
[2] E-mail: kopeika@bguee.bgu.ac.il.

1077-3169/97 $25.00

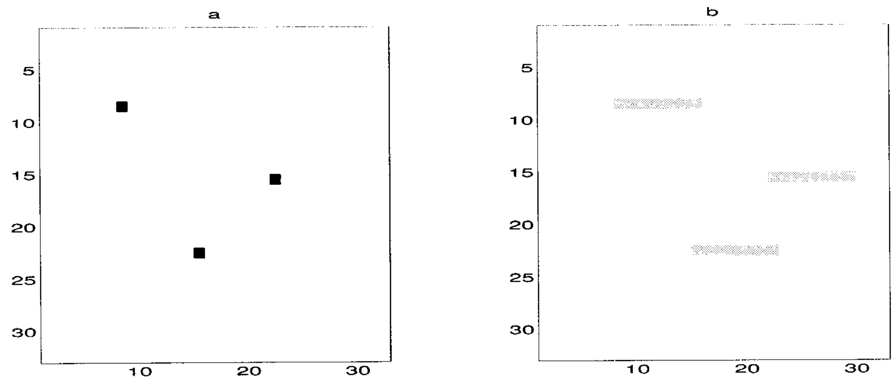

FIG. 1. (a) A 3-pixel image; (b) The blurred image using an 8-pixel square function.

the original image is assumed to be a stationary random process. These assumptions are very common in dealing with practical image restoration algorithms [1, 2, 4, 8, 11].

2. IDENTIFICATION OF BLUR PARAMETERS

In this chapter we present a method using the blurred image for identifying parameters of the blur caused by motion. First we describe the blur in the spatial domain followed by application to real world images. According to the characterizations of the blur effect we present in the third subsection a method for identifying the blur direction in the image. This is the first step in the identification algorithm described in the following subsection.

2.1. *Characterization of the Blur Effect*

As a result of relative motion between the camera and the object of interest, adjacent points in the image plane are exposed to the same point in the object plane during the exposure time. The intensity of an image of an original point is shared between these image plane points according to the relative duration in which each point was exposed to light from the original point. The smearing tracks of the points determine the PSF in the blurred image.

Exposure time is usually a fraction of a second (in real time imaging about 1/30). In many cases, there are no extreme changes in motion velocity during exposure time. In these cases extreme changes do not occur in the PSF shape. When the objects are distinct from their surrounding background, the smears can look like distinct tracks. For an evaluation of the homogeneity of these tracks we will define a *relative homogeneity* of a smear track of an image point as the ratio $d1/d2$, where:

—$d1$ is the minimum difference between the values of the pixels at the endpoints of the smear track of the point (the first and the last pixels) and the adjacent pixels outside the track.

—$d2$ is the maximum difference between two adjacent pixels inside the track.

According to this definition, when the relative homogeneity is high, a derivative of a blurred image along the tracks of the smear (i.e., the motion direction) will suppress the homogeneous area inside the tracks and emphasize their edges. The track derivative at its edges will usually have opposite signs. As a result of these properties of the image derivative, when a derivative followed by an autocorrelation operation is carried out in the motion direction, a minimum can be expected in the autocorrelation function (ACF) of the image derivative at a distance of the blur extent from the zero-shift center of the function. A simple illustration using an image of 3 pixels against a homogenous background is given in Fig. 1. This image is designate to clarify the above operations. However, it is certainly not characterized by real world image properties. The three pixel image of Fig. 1a was blurred by a horizontal square function of 8 pixels (uniform motion function) as shown in Fig. 1b. The values of the pixels inside a smear track are the same, as occurs with uniform motion, because the point spread or blur function is a one dimensional pulse of uniform height. The horizontal image derivative is shown in Fig. 2. Since the difference between two adjacent

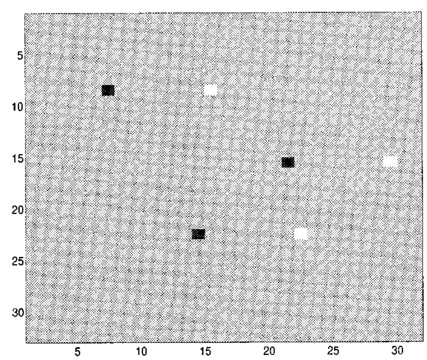

FIG. 2. The horizontal derivative of the blurred image of Fig. 1b.

pixels in a smearing track is zero, the derivative inside the track is zero. However, the derivatives at the edges of the smear have opposite signs (as in the derivative of a pulse). An autocorrelation of row 15 in the image derivative is shown in Fig. 3. Each minimum of this symmetric function is located 8 pixels from the center; i.e., an 8-pixel blur extent was identified by this ACF. In the case of the 3-pixel image, the relative homogeneity needed for identification of the blur extent is greater than unity. The reason is the shape of the ACF in this example is similar to the shape of the ACF of the PSF derivative. If we assume a unity *relative homogeneity* (i.e., the PSF is characterized by $d1 = d2$), the PSF derivative will have two minima (or maxima), both lowest (or highest) and equal to $d1$ and $d2$, one at distance of the blur extent, and the other located where $d2$ occurs. Therefore, the autocorrelation will also have two equal lowest minima at the same distances from its zero-shift point. If the relative homogeneity is lower than unity the global minimum of the ACF of the PSF derivative will be located where $d2$ occurs.

2.2. *Application to a Real Image*

In the case of a real life image the smear tracks of the points in the motion direction merge into each other. The values of $d1$ and $d2$ are then different from one pixel smear to the other since the background surrounding each pixel is different. Therefore, the contribution of each smear track to the shape of the ACF is different. On the other hand the motion blur has the same effect on all the points and, therefore, the effect of the blur on the ACF is cumulative, while the effect of the image derivative architecture is less meaningful since different architectures around each image derivative point cause a cancellation of their effects on the ACF, one by the other. In other words, the shape of the average of the ACFs of the image derivative lines along the motion direction will resemble the ACF of the PSF derivative.

Furthermore, since correlation in the original image exists in all directions, derivative of the image perpendicular to the motion direction decreases the correlation in the blurred image stemming from original image properties. Such operation does not have a meaningful effect on the blur characteristics in the blurred image since the blur is not correlated perpendicular to the motion direction. Therefore, as a result of this addition operation, the ACF is less affected by original image correlation properties.

As a result of the extreme suppression of the original image correlation properties by the derivative operations, the averaged ACF describes in particular the correlation properties of the PSF derivative. If the original image correlation properties are totally removed, the shape of the ACF of the image derivative is similar to the shape of the ACF of the PSF derivative and, therefore, the relative homogeneity of the PSF needed for identification of the blur extent would be greater than unity as explained at the end of Section 2.1. This condition can be shown by applying the method to different images blurred by accelerated motion PSFs forming different relative homogeneity values. An example of this is presented in Section 4.1.

The resemblance between the ACF of the blurred image derivative and that of the PSF derivative can still be observed when the relative homogeneity of the PSF is less than one, but in this case the global minimum of the ACF will not determine the blur extent since the global minimum of the PSF derivative ACF itself (the ideal result) is not located at the blur extent distance, as explained at the end of Section 2.1. Some examples for this resemblance are presented in Section 4.3.

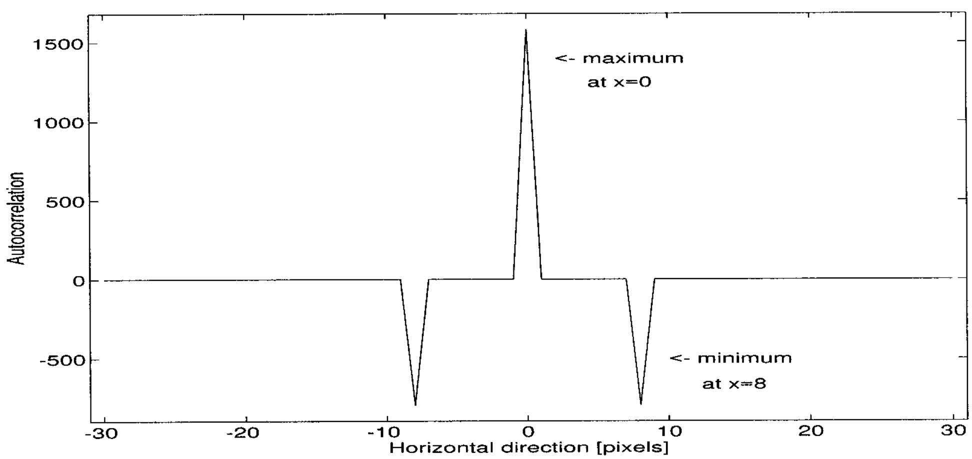

FIG. 3. The ACF of row 15 in the image derivative of Fig. 2. The blur extent (8 pixels) is equal to the location of the minimum of the function relative to the center.

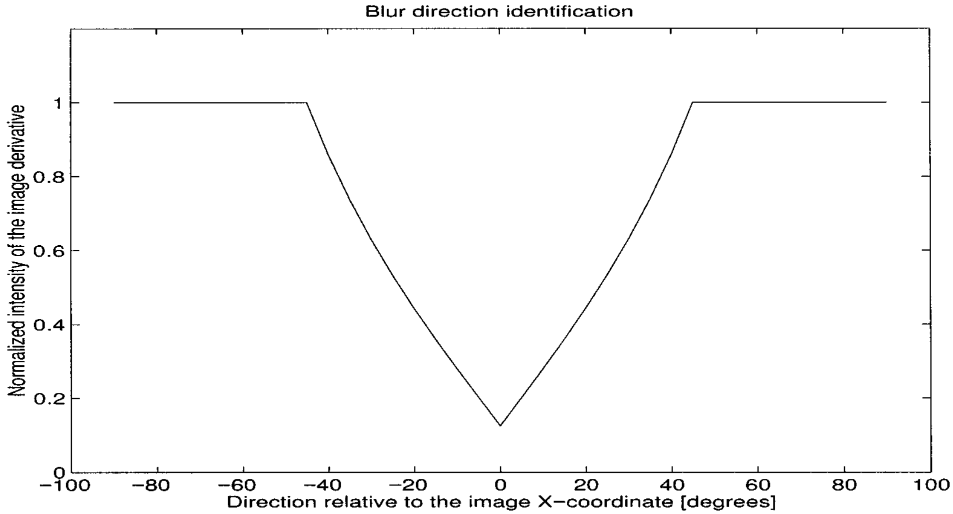

FIG. 4. The motion direction identification for the 3-pixel image.

2.3. *Identification of the Motion Direction*

The first necessary step of the method should be identification of the motion direction relative to the image axis. Extensive studies of image power spectra show that an excellent simple model for imagery statistics is that of a spatially isotropic first-order Markov process [12]. Hence, the autocorrelation of the original image and its power spectrum are assumed to be aproximately isotropic. As a consequence of motion, image resolution is decreased mostly in the motion direction. In the spatial frequency domain the derivative operation suppresses the low frequency and increases the high frequency contents. Since the blurring effect occurs in the motion direction, the intensity at the low frequencies is increased and the intensity at the high frequencies is decreased in this direction relative to other directions in the blurred image. Thus, a derivative of the image in this direction should suppress more of the image intensity than a derivative in other directions. Therefore, motion direction is identified by measuring the direction where the power spectrum of the image derivative is lower.

Application of this to the horizontally blurred three pixel image is shown in Fig. 4 where the summation of the image derivative absolute value is minimal for the derivative performed in the horizontal direction.

2.4. *Formulation of the Method*

A discrete approximation of the horizontal derivative at the point $f(i, j)$ in the image, where i and j are the horizontal and vertical directions respectively, is

$$\Delta f(i,j)_{[0\,\text{degrees}]} = f(i+1,j) - f(i,j) \tag{2}$$

where $f(i+1, j)$ indicates the pixel horizontally adjacent to the pixel $f(i,j)$. The derivative in the k direction (relative to the horizontal positive direction), where $0 \geq k \geq -45_{\text{degrees}}$, may be approximated as

$$\Delta f(i,j)_{[k\,\text{degrees}]} = f(i',j') - f(i,j) \tag{3}$$

where $f(i', j')$ is a virtual pixel in a direction k degrees from the pixel $f(i, j)$ as illustrated in Fig. 5. The intensity of this pixel is composed of intensities from both $f(i+1, j)$ and $f(i+1, j+1)$ according to the area from them included in $f(i', j')$. For example, in the case of Fig. 5, assuming the pixel area is 1, the pixel $f(i', j')$ is composed of $1 - \tan(k)$ of $f(i+1, j)$ and $\tan(k)$ of $f(i+1, j+1)$. Therefore, the value of $f(i', j')$ will be:

$$f(i',j') = f(i+1,j) \times (1 - \tan(k)) + f(i+1,j+1) \times \tan(k). \tag{4}$$

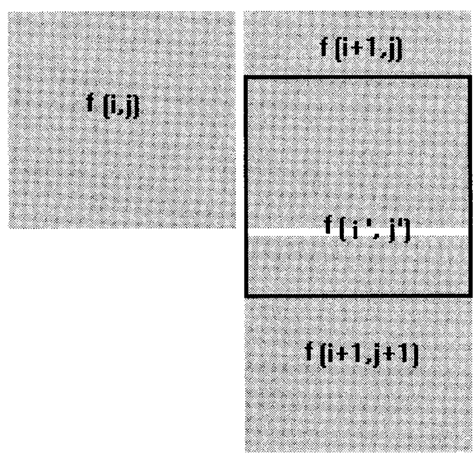

FIG. 5. The black frame indicates the 'pixel' $f(i', j')$.

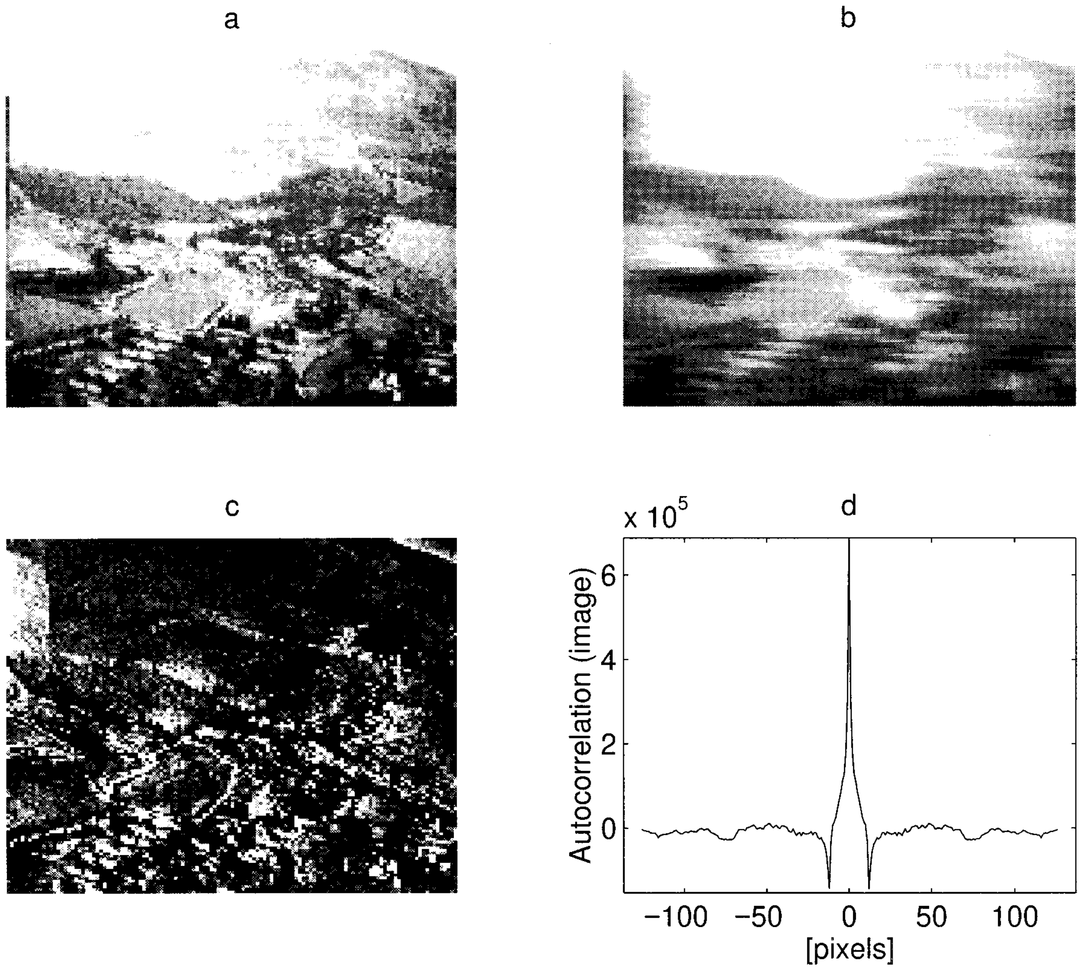

FIG. 6. Implementation for a real image. (a) The original *valley* image; (b) image blurred by horizontal accelerated motion function forming 12-pixel blur extent with 1.07 relative homogeneity of the PSF, and an additive zero mean normally distributed random noise causing 40 dB SNR; (c) the horizontal image derivative; (d) the average of the ACFs of the image derivative lines.

The image derivative approximation $\Delta f(i, j)$ in this direction will then be a convolution between the image $f(i, j)$ and a derivative operator.

$$\Delta f(i,j)_{k\,\text{degrees}} = f(i,j) \times D(i,j),$$
$$D(i,j) = \begin{bmatrix} -1 & 1-\tan(k) \\ 0 & \tan(k) \end{bmatrix}. \tag{5}$$

The total intensity of the image derivative $I(\Delta f)$ in this direction will be the summation of the absolute values of the pixels in $\Delta f(i, j)$,

$$I(\Delta f)_{k\,\text{degrees}} = \sum_{1}^{N-1} \sum_{1}^{M-1} |\Delta f(i,j)_{k\,\text{degrees}}|, \tag{6}$$

where M and N are the numbers of rows and columns in the image $\Delta f(i, j)$.

2.5. *Summary of the Identification Method*

(a) Motion direction k relative to the image axis is identified by measuring the direction where the total intensity of the image derivative (6) is lowest.

(b) In cases of images with low noise (SNR > 35 dB), derivatives of the blurred image both perpendicular to and in the motion direction are computed according to (5). For relatively noisy images, only a derivative in the motion direction is computed.

(c) A digital ACF to the image derivative lines in the motion direction is calculated, where ACF $R_l(j)$ of an M-pixel image derivative line l is defined as

$$R_l(j) = \sum_{i=-M}^{M} l(i+j)l(i) \quad \text{integer}\, j \in [-M, M] \tag{7}$$
$$\text{where } l(i) = 0 \quad \text{for } (i) \notin [0, M].$$

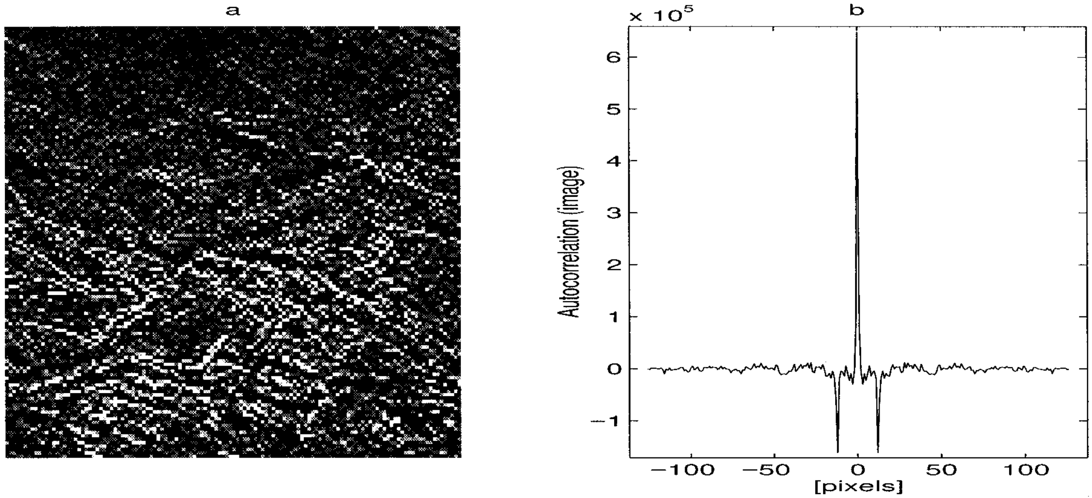

FIG. 7. (a) The horizontal derivative of the vertical derivative of the blurred valley image; (b) the average of the ACFs of the image derivative lines of (a).

The results of these steps are identification of the direction of motion k and the average of the ACFs of the image derivative lines $\overline{R}_{\Delta f}$. The blur extent is the distance between the location of the minimum of $\overline{R}_{\Delta f}$ and its zero-shift point $\overline{R}_{\Delta f}(0)$. The shape of $\overline{R}_{\Delta f}$ characterizes the shape of the ACF of the PSF derivative as discussed later. As a result of the discrete nature of the image, resolution of the identified blur extent is limited by the distance between two adjacent pixels.

3. IDENTIFICATION RESULTS

3.1. *Synthetic Blur*

The original *valley* image in Fig. 6a was blurred by a horizontal accelerated motion function of 12 pixels forming a 1.07 *relative homogeneity* of the PSF, and an additive zero mean normally distributed random noise causing 40 dB SNR, as shown in Fig. 6b. The horizontal image derivative is presented in Fig. 6c and the average of the ACFs of the image derivative lines is shown in Fig. 6d. The 12-pixel blur extent is identified by the location of the minimum of this function relative to its zero-shift point.

Figure 7a shows the blurred valley image derivative, after both horizontal and vertical derivative operations. The average of the ACFs of the image derivative rows appears in Fig. 7b. The minimum that is located at the distance of the blur extent from the center of this function is sharper than the one achieved in Fig. 6d, where only a horizontal derivative was carried out, and the shape of the function is much more similar to the shape of the PSF derivative.

3.2. *Real Camera Motion Blur*

The blurred image *phone* that is presented in Fig. 8a was mechanically vibrated horizontally using an experimental setup with a chemical shaker as described in Ref. [4]. The

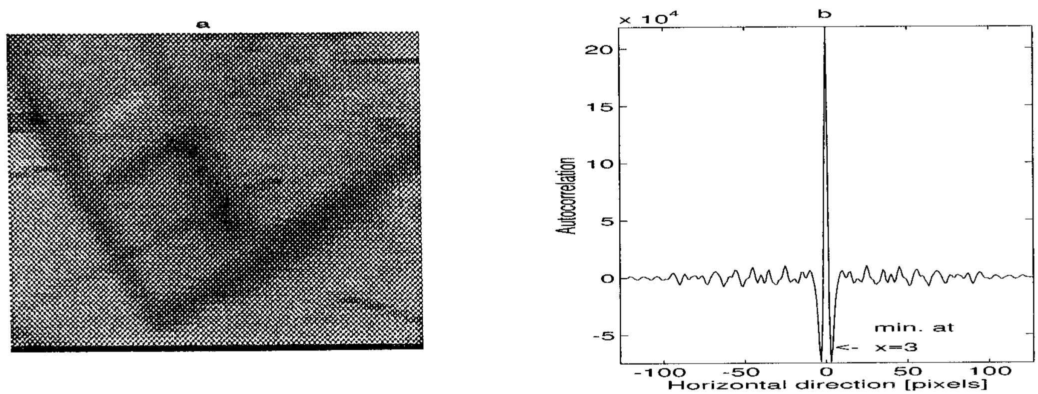

FIG. 8. (a) The image *phone* mechanically blurred horizontally by low frequency vibrations; (b) a 3-pixel blur extent was identified by a clear minimum in the identification function.

FIG. 9. The restored phone image using a Wiener filter assuming a 3-pixel square function PSF.

identification result presented in Fig. 8b shows clearly a 3-pixel blur extent. Figure 9 shows a restoration of the image using a simple Wiener filter [10, 11] and a 3-pixel square function assumed for PSF.

The image in Fig. 10 was blurred by manual motion of the camera. A function of the image derivative intensity (6) in all directions relative to the x-coordinate is presented in Fig. 11a and the minimum appears at 55°. The resulting ACF presented in Fig. 11b identifies a blur extent of 18 pixels. Figure 12 show a restoration of the image using a simple Wiener filter with an 18-pixel square function PSF corresponding to uniform velocity. The image in Fig. 13 was also manually blurred by moving the camera. The function in Fig. 14a shows a minimum at 0° which indicates that the motion blur was in this direction. The resulting autocorrelation presented in Fig. 14b identifies a blur extent of 8 pixels. A restoration result using a Wiener filter is presented in Fig. 15.

3.3. *Evaluation of PSF Shape*

The resemblance that should appear using the function obtained from the identification method and the autocorrelation of the blurring PSF derivative was explained in Section 2.2. In Fig. 16 we can see results of the method for different types of simulated common motion blurs performed on the valley image of Fig. 6a. In Figs. 16.a1–c1 we see the PSFs used to blur the image: (a1) PSF for temporal uniform motion, (b1) PSF for accelerated motion, and (c1) PSF for high temporal frequency vibrations. Figs. 16.a2–c2 show the ACFs of the derivatives of these PSFs respectively (the ideal identification results). Figs. 16.a3–c3 present the average of the ACFs of the blurred image derivative lines for each case and we can see that these identification results are similar to the ideal ones.

4. DISCUSSION

4.1. *Capability of the Identification Method Concerning Common Motion Types*

The capability of the blur parameter identification depends mainly on the relative homogeneity of the blurred image objects tracks. The capability of the method is increased when the relative homogeneity of the PSF is higher. In the case of uniform motion, the relative homogeneity $d1/d2$ of the PSF is infinity, and therefore identification capability is very high. For constant acceleration motion, the relative homogeneity of the PSF is higher when the acceleration is lower and the initial velocity is higher [3].

Another common source of blur is sinusoidal motion (vibration). This motion type can be divided into two types: low and high temporal frequency vibrations. Vibrations are defined as high frequency when the exposure time is

FIG. 10. An image manually blurred by motion of the camera.

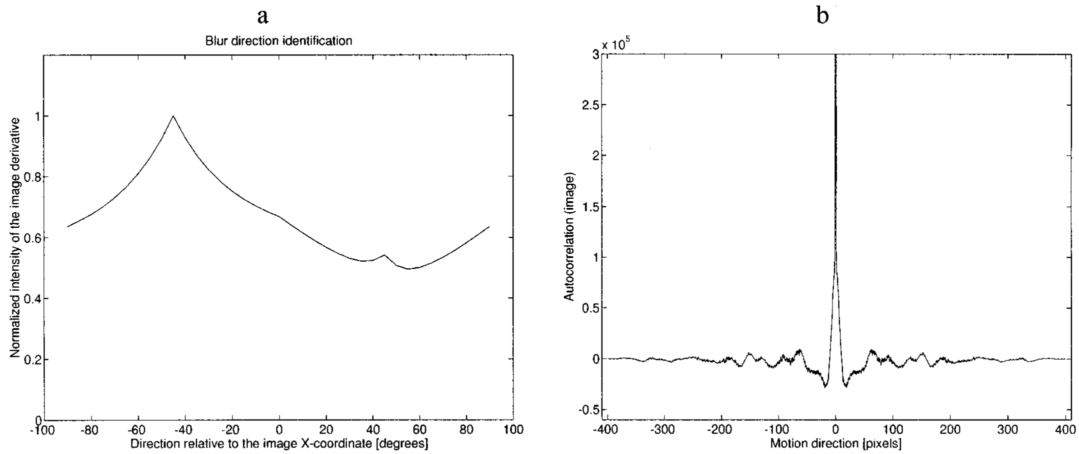

FIG. 11. (a) The motion direction (55°) is indicated by the location of the minimum in the motion direction identification function; (b) 18 pixels blur extent is identified by the ACF of the blurred image derivative.

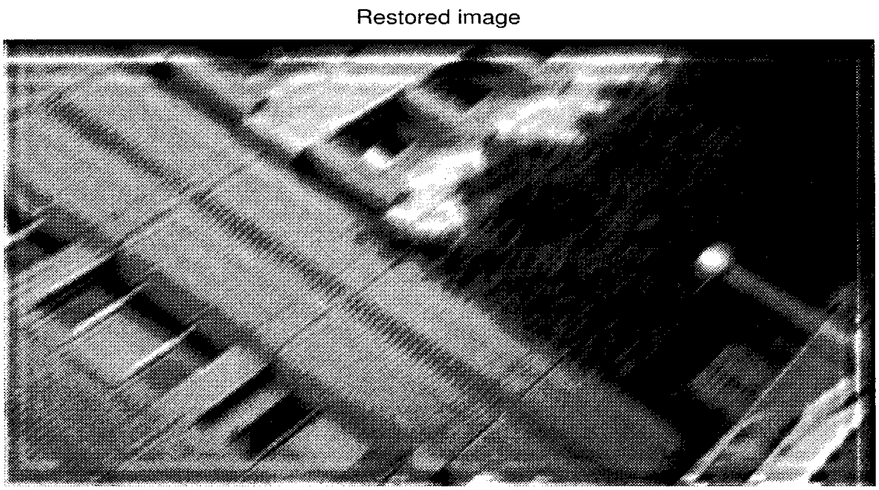

FIG. 12. Restored image using the identified parameters in the Wiener filter.

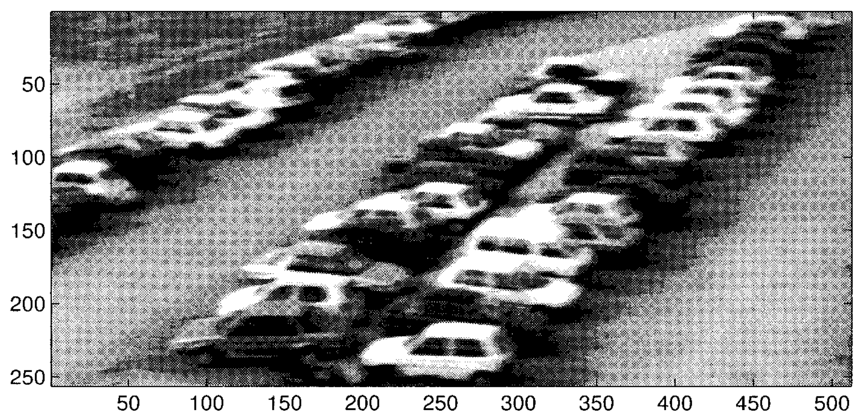

FIG. 13. An image manually blurred by motion of the camera.

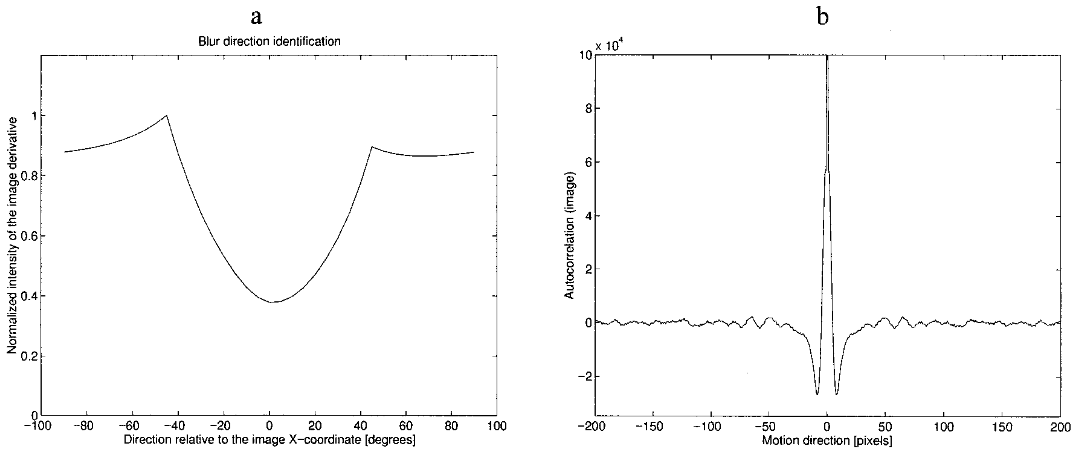

FIG. 14. (a) Zero degrees motion direction is identified in the direction identification function; (b) 8 pixels blur extent is identified by the ACF of the blurred image derivative.

longer than the time period of the vibration, and as low frequency when the opposite is true. The PSF of high frequency vibrations can be determined only by the blur extent. The line spread function (LSF) in this case is $1/\pi(D^2 - x^2)^{1/2}$, where D is the blur extent and $|x| < D$ [4]. The relative homogeneity in this case is high enough for clear identification of the blur extent.

For low-frequency vibrations a large variety of PSF shapes can occur, depending on the portion of the vibration period in which exposure time is included [4]. The LSF here is, in general, a portin of the high-frequency vibration LSF and can be determined uniquely by the exposure time, the time period, and the blur extent. Therefore, if the first two parameters are known, identification of the blur extent can be used to determine the portion of vibration where exposure occurred, and this lead to identification of the motion LSF. The relative homogeneity in this case naturally depends on the sine wave vibration portion in which exposure take place, and the proposed method can identify the blur extent for most of the portions. As exposure time is shorter, the relative homogeneity is higher for most of the cases since no extreme changes occur in the motion velocity during a small portion of the vibration period.

4.2. *Comparative Discussion*

Cannon's zero crossings identification approach [1] is also performed straightforwardly and separately from the restoration process, but the method we propose includes very different steps to suppress the effects of the original image and to enhance the effects of the PSF on the blur identification result. Two main drawbacks involved in Cannon's approach are addressed here: (a) no treatment concerning the PSF shape, which is considered here in Section 4.3; (b) the blur extent is restricted to be two orders of

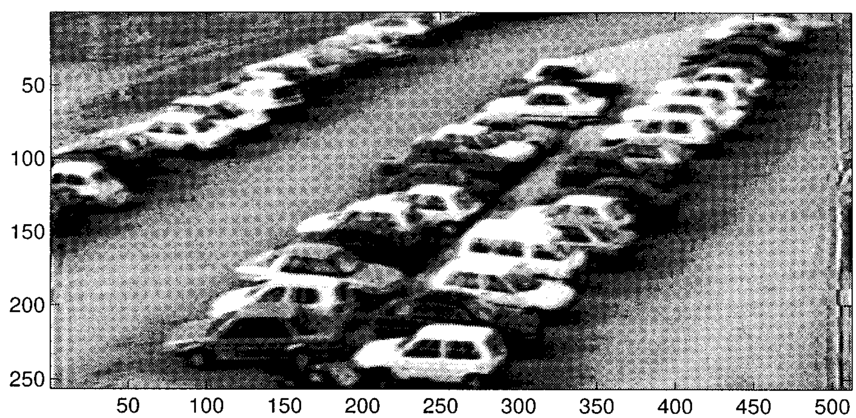

FIG. 15. Restored image using the identified parameters in the Wiener filter.

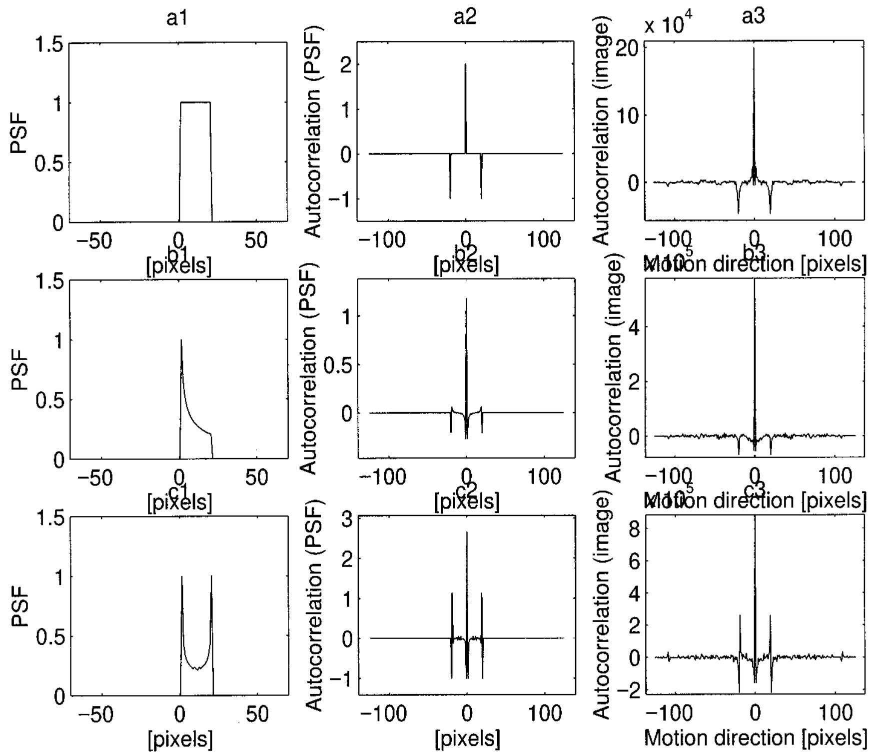

FIG. 16. Identification results for different motion types implemented on valley image. (a1, b1, c1) the blurring PSFs; (a2, b2, c2) the ACFs of the PSFs; (a3, b3, c3) the average of the ACFs of the blurred image derivative lines.

magnitude smaller than that of the image since, for the purpose of identification, the blurred image is broken up into many smaller images each of which is large enough to contain the unknown PSF. This restriction does not exist in the method proposed here since motion direction is identified first. Therefore, the blur extent can be up to half of an image line extent.

5. SUMMARY AND CONCLUSIONS

A method for identifying blur parameters from motion-blurred images is presented. The capability for correct and clear identification of the blur parameters depends mainly on the relative homogeneity determined in Section 2. When the relative homogeneity of the PSF is greater than unity, a correct identification can be carried out. The quality of the identification results is expressed by better resemblance between the obtained identification function and the autocorrelation of the true PSF derivative.

Since this method does not include an image restoration process with the identification process, restored image criteria are not included in the identification process considerations. If a criterion-based method for image restoration is to be carried out, the method proposed here can be used to provide the blur parameters with which to begin.

ACKNOWLEDGMENTS

The authors appreciate the support given by the Paul Ivanir Center for Robotics and Production Management at Ben Gurion University of the Negev, and the support of the Jacob Ben-Isaac Hacohen Fellowship to Mr. Y. Yitzhaky.

REFERENCES

1. M. Cannon, Blind deconvolution of spatially invariant image blurs with phase, *IEEE Trans. Acoust. Speech Signal Process.* **ASSP-24,** 1976.
2. S. C. Som, Analysis of the effect of linear smear on photographic images, *J. Opt. Soc. Am.* **61,** 1971, 859–864.
3. O. Hadar, S. R. Rotman, and N. S. Kopeika, Target acquisition modeling of forward-motion considerations for airborne reconnaissance over hostile territory, *Opt. Eng.* **33,** 1994, 3106–3117.
4. O. Hadar, I. Dror, and N. S. Kopeika, Image resolution limits resulting from mechanical vibrations. IV. Real-time numerical calculation of optical transfer function and experimental verification, *Opt. Eng.* **33,** 1994, 566–578.
5. A. K. Katsaggelos, Ed., *Digital Image Restoration,* Springer-Verlag, New York, 1991.
6. R. L. Lagendijk, A. M. Tekalp, and J. Biemond, Maximum likelihood image and blur identification: A unifying approach, *Opt. Eng.* **29,** 1990, 422–435.
7. G. Pavlovic and A. M. Tekalp, Maximum likelihood parametric blur identification based on a continuous spatial domain model, *IEEE Trans. Image Process.* **1,** 1992.

8. A. E. Savakis and H. J. Trussell, Blur identification by residual spectral matching, *IEEE Trans. Image Process.* **2,** 1993, 141–151.
9. P. D. Welch, The use of the fast Fourier transform for the estimation of power spectra: A method based on time averaging over short, modified periodograms, *IEEE Trans. Audio Electroacoust.* **AU-15,** 1967, 70–73.
10. H. Lim, K. C. Tan, and B. T. G. Tan, Edge errors in inverse and Wiener filter restorations of motion-blurred images and their windowing treatment, *CVGIP: Graph. Models Image Process.* **53,** 1991, 186–195.
11. A. Rosenfeld and A. C. Kak, *Digital Picture Processing,* Vol. 2, Academic Press, New York, 1982.
12. M. P. Ekstrom, Ed., *Digital Image Processing Techniques,* Academic Press, Orlando, FL., 1984.